Materials Research Proceedings **26** (2023) 287-292 https://doi.org/10.21741/9781644902431-47

A limit analysis approach for the prediction of the human proximal femur ultimate load

Aurora Angela Pisano[1,a*], Paolo Fuschi[1,b]

[1]University Mediterranea of Reggio Calabria, Reggio Calabria, Italy

[a]aurora.pisano@unirc.it, [b]paolo.fuschi@unirc.it

Keywords: Static Limit Analysis, Human Proximal Femur, Tsai-Wu Constitutive Criterion

Abstract. A limit analysis numerical procedure for the determination of a lower bound on the ultimate load of the human proximal femur is presented. The procedure, already applied by the authors in different contexts, is based on a simplified 3D geometrical model of the human femur and on the assumption of a few geometric and material data available in the relevant literature. The perfectly plastic behaviour of the human bone, due to phenomena starting at molecular scale, and the orthotropic behaviour of the main human femur tissues, *trabecular* and *cortical*, allows to assume a yield surface of Tsai-Wu-type for its constitutive description. The effectiveness of the promoted numerical approach is validated by comparison of the obtained results with experimental findings on in-vitro tests of human femurs.

Introduction

The limit analysis theory, in a numerical formulation oriented to the determination of a lower bound to the collapse load of a structural element and already employed by the authors for the solution of several engineering structural problems [1] is applied in the context of human long bones. The study is focused on of the collapse load of the human proximal femur and this, in the spirit of the static approach of the limit analysis theory, without following the load history that has produced it, excluding as well all the post elastic phenomena, damage or fracture propagation in the bone.

In the promoted approach, the main pre-collapse phenomenon arising within the human bone material, that is the stress redistribution process, is numerically simulated by means of an appropriate adjustment of the elastic moduli of the main constituent materials of the bone, namely the cortical and the trabecular bone tissues. For both the above main constituents it is assumed a criterion of Tsai-Wu-type formulated in principal stress space which, in the 3D context, proves to be a strictly convex domain for the admissible stresses. The few material parameters needed to define the constitutive criterion and to carry on the whole limit analysis procedure represents a very attractive feature of the proposed method which can be easily connected with molecular imaging and/or other diagnostic tools of prevention.

The simulation of the stress redistribution process, arising within the bone element until collapse, is carried on iteratively with reference to a simplified model of the proximal human femur, which approximate the geometry of the bone and that, discretized in 3D solids finite elements, is used to analyse two well known mechanical configurations producing the human proximal femur collapse, i.e. the so-called stance and side configurations, [2,3]. The former is aimed to predict bone fracture under single-leg-stance loading, the latter under sideways-fall.

Few numerical examples are carried out for comparison with the results of experimental tests available in the relevant literature for in-vitro tests on human femurs, [3], also with the purpose to define the sensitivity of the results by varying some geometric and material parameters. The obtained numerical findings definitively show a good capacity of the employed numerical method to predict the real limit load of the proximal human femur under prescribed load conditions.

Materials Research Proceedings **26** (2023) 287-292 https://doi.org/10.21741/9781644902431-47

Theoretical background

The static approach of limit analysis theory, as said in the introductory section, is aimed to the determination of a lower bound to the collapse load of a structure or of a structural element. This goal is classically pursued by applying the Lower-Bound Theorem of limit analysis that leads to a maximization problem in which, a fixed reference load distribution, defining the loading conditions, is amplified by a single scalar load multiplier, say P_{LB}, that produces loads that are in equilibrium with a stress field, that nowhere violates the yield criterion of the constituent material, and that do not exceed the effective collapse load multiplier, say P_U . P_{LB} is then a Lower Bound (LB) to the load multiplier whose maximum, obtainable by increasing the acting loads, defines the collapse, or peak, load value of the structure. It is worth to remind that no matters the elastic behaviour before collapse or any type of elasticity law followed by the constituent material.

On the other hand, the existence of a yield criterion for bone material is assured by the circumstance that plasticity in bones starts at molecular scale and is due to breaking of hydrogen bonds within single collagen molecules followed by breaking of bonds and intermolecular sliding within collagen fibrils, see e.g. [4]. The irrelevance of the elastic behaviour before collapse is a key point for the numerical procedure hereafter promoted, namely the Elastic Compensation Method (ECM) [1,2]. Indeed, the ECM varies, within a discretized FE model of the bone, the elastic moduli of the "bone material" to simulate the process of stress re-distribution arising within the bone suffering an increasing load until the attainment of its strength threshold.

Limit analysis on human proximal femur

The simplified geometrical model of Fig.1 has been assumed for the human proximal femur. The external dimensions of the bone, borrowed from the relevant literature, are given in the same figure in tabular form.

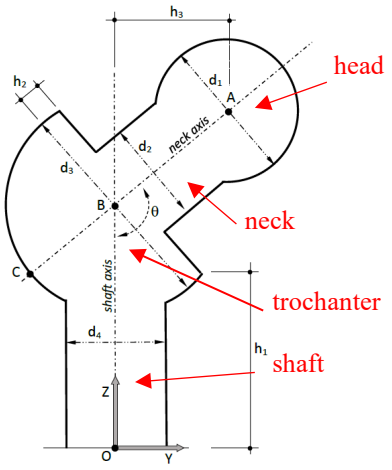

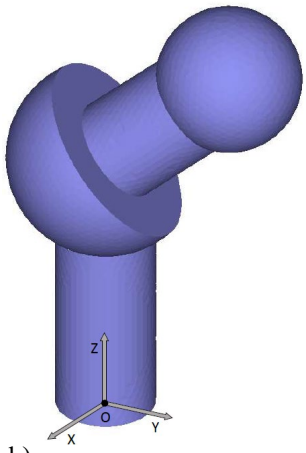

Dimension		Reference
d_1 [mm]	51.60	[5]
d_2	37.40	[5]
d_3	65.64	[6]
d_4	35.40	[6]
h_1	80.00	[3]
h_2	5.30	[6]
h_3	44.00	[6]
AC	90.26	[6]
θ [grad]	130	[7]

***Figure 1**. Human proximal femur model: a) geometry referred to the medio-lateral section; b) 3D model and main reference orthogonal coordinate system; dimensions taken from the relevant literature in tabular form.*

It should be specified that the bone has an external part made of cortical tissue and an internal part made of trabecular and marrow tissues, the latter is only present in the shaft zone. The thickness of the cortical tissue is here considered variable in the different zones into which the simplified proximal femur model has been divided. In particular, from now on S1, S2 and S3

Materials Research Proceedings **26** (2023) 287-292 https://doi.org/10.21741/9781644902431-47

indicate the cortical thickness in the head zone, in the neck and trochanter zones and in the shaft zone, respectively.

As already said, the cortical and trabecular tissues are assumed to obey a Tsai-Wu-type constitutive criterion, which in principal stress space can be given the shape:

$$G_{11}\sigma_{11}+G_{22}\sigma_{22}+G_{33}\sigma_{33}+F_{1111}\sigma_{11}^2+F_{2222}\sigma_{22}^2+F_{3333}\sigma_{33}^2+ 2F_{1122}\sigma_{11}\sigma_{22}+2F_{1133}\sigma_{11}\sigma_{33}+2F_{2233}\sigma_{22}\sigma_{33}=1 \quad (1)$$

where:

$$G_{ii}=\frac{1}{\sigma_i^+}-\frac{1}{\sigma_i^-};\quad F_{iiii}=\frac{1}{\sigma_i^+\sigma_i^-};\quad F_{iijj}=\frac{1}{2}\left(\frac{1}{\sigma_i^+\sigma_i^-}+\frac{1}{\sigma_j^+\sigma_j^-}-\frac{1}{\sigma_{ij}^2}\right) \quad (2)$$

In Eq.(1) σ_{11}, σ_{22}, σ_{33} are principal stresses and repeated indices in Eqs.(2) do not imply summation. Moreover, σ_i^+, σ_i^-, σ_{ij} are the moduli of ultimate strengths in tension, compression and shear, respectively; finally i, j=1, 2, 3 refer to direction and plane of orthotropy.

Typical Tsai-Wu-type yield surfaces for the two main bone tissues are shown in Fig.2 and the ECM limit analysis procedure is applied with reference to both these yield surfaces.

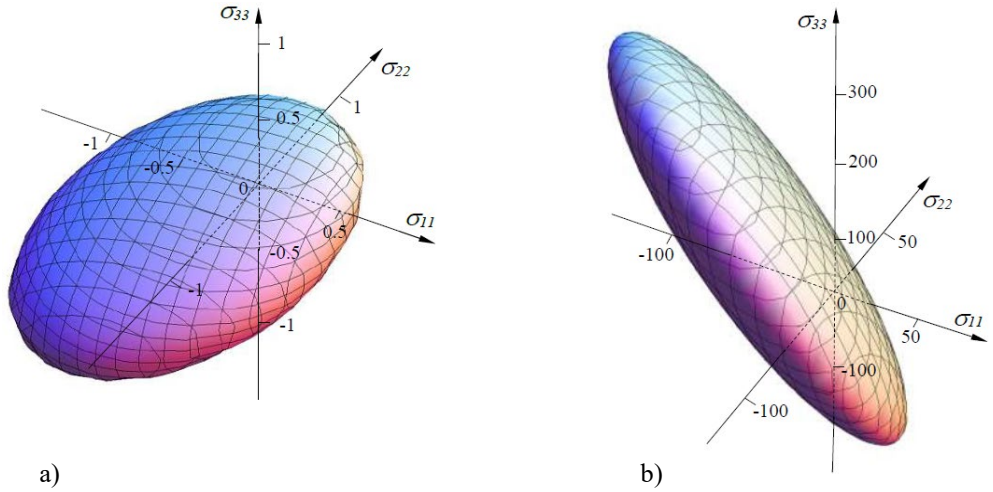

a) b)

***Figure 2**. Typical Tsai-Wu-type yield surface for trabecular a) and cortical b) proximal femur tissues.*

For sake of brevity, the Reader can refer to [1,2] for the details on the ECM iterative procedure. The latter performs a sequence of FE elastic analyses and, within each sequence carried on for a fixed loads distribution, applies an iterative procedure. It is worth noting that, at current iteration, the elastic moduli within the discretized structural model, are updated (reduced) only within those FEs where the elastic element solution, in terms of average stress within the element, is "greater" than the corresponding stress at yield. This produces, at the subsequent iteration (within the current sequence of elastic FE analyses), a redistribution of the stresses, which migrate from the weakened elements to the neighbour ones, so miming the redistribution of the stresses arising before the incipient state of collapse. The latter is reached when, for the applied loads (increased sequence by sequence by increasing the acting loads multiplier), such redistribution is not possible any more.

In-silico *vs* in-vitro tests

Two experimental tests on real human proximal femurs, after D'Allara et al. 2013, [3], have been numerically reproduced, precisely, the so-called STANCE and SIDE configurations which are shown in Fig.3(a-c) together with the assumed FE models.

Materials Research Proceedings **26** (2023) 287-292 https://doi.org/10.21741/9781644902431-47

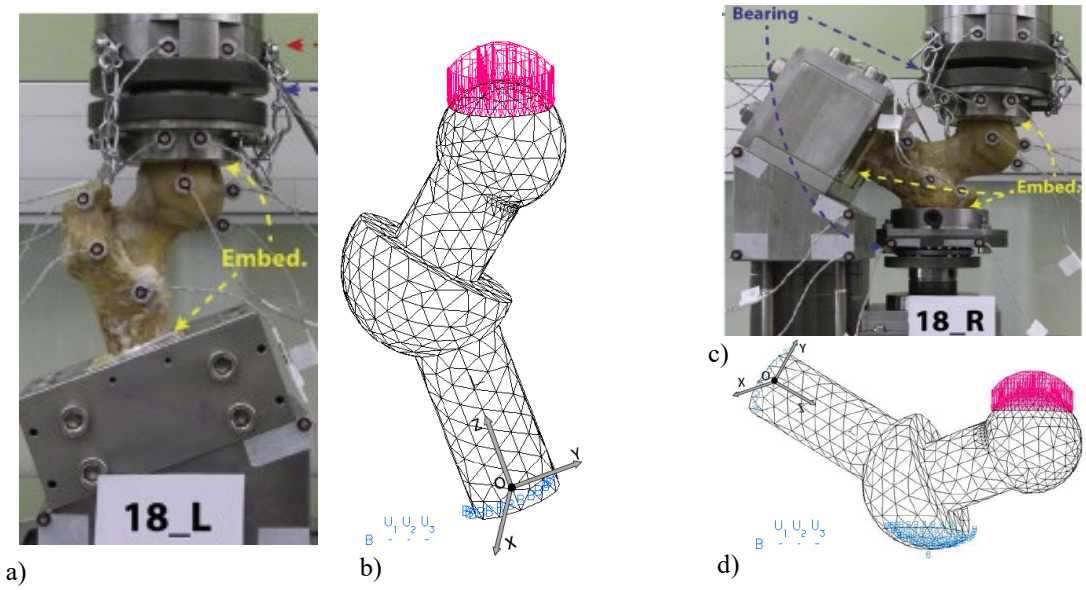

Figure 3. *Human proximal femur in-silico configurations: STANCE a) Experimental set up (after [3]), b) FE mesh of 6408 3D-Solids (10nodes, 17GPs); SIDE c) Experimental set up (after [3]), d) FE mesh of 7111 3D-Solids (10nodes, 17GPs)*

In order to evaluate the influence on the collapse load of material and geometric parameters, three different material strength values (for cortical and trabecular) and three different geometrical models have been considered and this for each configuration, STANCE and SIDE.

Three pairs of apparent density values are assumed leading to the definition of three different materials, hereinafter referred to as Mat_1, Mat_2 and Mat_3. In particular, for Mat_1 $\rho_{cortical} = 1.5$ g/cm^3 and $\rho_{trabecular} = 0.1$ g/cm^3; for Mat_2 $\rho_{cortical} = 1.75$ g/cm^3 and $\rho_{trabecular} = 0.4$ g/cm^3 ; finally for Mat_3 $\rho_{cortical} = 2.0$ g/cm^3 and $\rho_{trabecular} = 0.7$ g/cm^3. These values, corresponding to the minimum, average and maximum values of apparent density either in cortical and in trabecular, give rise to the strength material values reported in Table1. Finally, the contribution of the marrow to the overall strength of the femur is neglected.

Concerning the geometry, three geometrical models, hereinafter named GM_1, GM_2 and GM_3, are obtained by assuming for the thickness of the cortical in the shaft (S3) the values 5.7 mm, 7 mm and 8.3 mm, respectively. Moreover, following [16] the thickness in other zones of the bone are derived by assuming the ratios S1 / S2 = 0.5 and S1 / S3 = 0.25. In summary, the adopted ECM FE-based numerical predictive procedure has been applied nine times for each configuration.

The obtained results, in terms of P_{LB} are reported in Table 2. It can be observed that for fixed geometry (values reported in columns) there is a great variability of the P_{LB} as the strength characteristics of the material vary, while the variability for fixed material strengths (values reported in rows) is less relevant on varying the geometry. It is then essential to calibrate the strength parameters as accurately as possible to increase the predictive capabilities of the whole procedure. Another important remark is that the ECM is able to reproduce the experimental data and, in fact, for the average value of $\rho_{cortical}$, corresponding to the row Mat_2, the values of the collapse loads are very close to each other and to the ones given in the quoted experiments. More precisely, in the STANCE configuration the experimental collapse load value is 8.7 ± 2.9 kN and the one obtained from the numerical simulations is 9 ± 1.5 kN, in the SIDE configuration the experimental collapse load is 3.1 ± 1.1 kN and the one obtained applying the ECM procedure is 4 ± 0.5 kN.

Materials Research Proceedings **26** (2023) 287-292 https://doi.org/10.21741/9781644902431-47

***Table 1**. Assumed strength values [MPa] for the two main bone tissues.*

Strength	Cortical	Trabecular	Cortical	Trabecular
	Mat_1		Mat_2	
$\sigma_1^- = \sigma_2^-$	$68.249^{(1)}$	$0.913^{(1)}$	$86.137^{(1)}$	$6.099^{(1)}$
σ_3^-	$155.164^{(1)}$	$0.526^{(1)}$	$207.324^{(1)}$	$7.220^{(1)}$
$\sigma_1^+ = \sigma_2^+$	$23.887^{(2)}$	$0.602^{(3)}$	$30.148^{(2)}$	$4.025^{(3)}$
σ_3^+	$93.098^{(4)}$	$0.347^{(5)}$	$124.394^{(4)}$	$4.765^{(5)}$
$\sigma_{13} = \sigma_{23}$	$53.50^{(6)}$	$0.315^{(7)}$	$53.50^{(6)}$	$4.332^{(7)}$
σ_{12}	$67.80^{(6)}$	$0.548^{(8)}$	$67.80^{(6)}$	$3.659^{(8)}$
	Mat_3		Reference	
$\sigma_1^- = \sigma_2^-$	$105.380^{(1)}$	$13.128^{(1)}$	[8,9,10] (1)	
σ_3^-	$266.486^{(1)}$	$20.792^{(1)}$		
$\sigma_1^+ = \sigma_2^+$	$36.883^{(2)}$	$8.664^{(3)}$	[11,12] (2)	($\sigma_1^+ = \sigma_2^+ = 35\% \sigma_1^-$)
			[13] (3)	($\sigma_1^+ = \sigma_2^+ = 66\% \sigma_1^-$)
σ_3^+	$159.892^{(4)}$	$13.722^{(5)}$	[11,12] (4)	($\sigma_3^+ = 60\% \sigma_3^-$)
			[13] (5)	($\sigma_3^+ = 66\% \sigma_3^-$)
$\sigma_{13} = \sigma_{23}$	$53.50^{(6)}$	$12.475^{(7)}$	[14] (6), [15] (7)	($\sigma_{13} = \sigma_{23} = 0.6 \sigma_3^-$)
σ_{12}	$67.80^{(6)}$	$7.877^{(8)}$	[15] (8)	($\sigma_{12} = 0.6 \sigma_1^-$)

***Table 2**. P_{LB} values for the three geometrical models (GM_1, GM_2, GM_3) and for the three considered materials (Mat_1, Mat_2, Mat_3): a) STANCE configuration, b) SIDE configuration.*

Geometrical Model/ Material Model	GM_1	GM_2	GM_3
Mat_1	3	3.5	5
Mat_2	7.5	9	10.5
Mat_3	14	17	18

a)

Geometrical Model/ Material Model	GM_1	GM_2	GM_3
Mat_1	1.7	2.2	2.7
Mat_2	3.5	4	4.5
Mat_3	6.2	7	7.3

b)

Concluding remarks

The numerical iterative procedure, known in the literature as Elastic Compensation Method, has been applied to determine a lower bound on the ultimate load of the human proximal femur. The specification of a few geometrical and material parameters suffices to reach a very good prediction of the ultimate load. In particular, rather than the geometrical parameters, the needed crucial parameters are the strengths of the cortical and trabecular tissues, which are related to the bone mineral density. The obtained results seem very promising as witnessed by comparison with available experimental data on the collapse load of in-vitro specimens for two typical conditions driving to human femur rupture. On taking into account that the bone mineral density and, in general, the actual bones' strengths of a patient affected by orthopedic diseases are nowadays easily detectable via molecular imaging, a predictive tool as the one here promoted could be easily

integrated within diagnostic tools of prevention.

References

[1] A.A. Pisano, P. Fuschi, D. De Domenico. Numerical limit analysis of steel-reinforced concrete walls and slabs, Computers and Structures, 160, 42-55, (2015). https://doi.org/10.1016/j.compstruc.2015.08.004

[2] A.A. Pisano, P. Fuschi. Limit Analysis of Human Proximal Femur. Journal of the Mechanical Behavior of Biomedical Materials. 124, 104844, (2021). https://doi.org/10.1016/j.jmbbm.2021.104844

[3] E. Dall'Ara, B. Luisier , R. Schmidt, M. Pretterklieber, F. Kainberger, P. Zysset , D. Pahr. DXA predictions of human femoral mechanical properties depend on the load configuration, Medical Engineering & Physics, 35, 1564-1572, (2013). https://doi.org/10.1016/j.medengphy.2013.04.008

[4] R.O. Ritchie, M.J. Buehler, P. Hansma. Plasticity and toughness in bone, Physics Today, 62(6), 41-47, (2009). https://doi.org/10.1063/1.3156332

[5] G. Holzer, G. von Skrbensky, L.A. Holzer, W. Pichl. Hip Fractures and the Contribution of Cortical Versus Trabecular Bone to Femoral Neck Strength, Journal of Bone and Mineral Research, 24(3), 468-474, (2009). https://doi.org/10.1359/jbmr.081108

[6] J. Michelotti, J. Clark. Femoral Neck Length and Hip Fracture Risk, Journal of Bone and Mineral Research, 14(10), 1714-1720, (1999). https://doi.org/10.1359/jbmr.1999.14.10.1714

[7] Z. Yang, W. Jian, L. Zhi-han, X. Jun, Z. Liang, Y. Ge, S. Zhan-jun. The Geometry of the Bone Structure Associated with Total Hip Arthroplasty. PLOS ONE, 9(3):e91058, doi: 10.1371/journal.pone. 0091058, (2014). https://doi.org/10.1371/journal.pone.0091058

[8] D.C. Wirtz, N. Schiffers, T. Pandorf, K. Radermacher, D. Weichert, R. Forst. Critical evaluation of known bone material properties to realize anisotropic FE-simulation of proximal femur, Journal of Biomechanics, 33, 1325-1330, (2000). https://doi.org/10.1016/S0021-9290(00)00069-5

[9] J.C. Lotz, T.N. Gerhart, W.C. Hayes. Mechanical properties of trabecular bone from the proximal femur: a quantitative CT study, Journal of Computer Assisted Tomography, 14, 107-114, (1990). https://doi.org/10.1097/00004728-199001000-00020

[10] J.C. Lotz, T.N. Gerhart, W.C. Hayes. Mechanical properties of metaphyseal bone in the proximal femur, Journal of Biomechanics, 24, 317-329, (1991). https://doi.org/10.1016/0021-9290(91)90350-V

[11] J. Currey. Cortical Bone. In: Handbook of Biomaterial Properties, (Chapter A1) Springer Science + Business Media New York 2016, W. Murphy et al. (eds.), (2016).

[12] M. Doblaré, J.M. García, M.J. Gómez. Modelling bone tissue fracture and healing: a review, Engineering Fracture Mechanics, 71, 1809-1840, (2004). https://doi.org/10.1016/j.engfracmech.2003.08.003

[13] L. Rincón-Kohli, P.K. Zysset. Multi-axial mechanical properties of human trabecular bone. Biomechanics and Modeling in Mechanobiology, 8(3), 195-208, (2009). https://doi.org/10.1007/s10237-008-0128-z

[14] C.H. Turner, T. Wang, D.B. Burr. Shear Strength and Fatigue Properties of Human Cortical Bone Determined from Pure Shear Tests, Calcified Tissue International, 69, 373-378, (2001). https://doi.org/10.1007/s00223-001-1006-1

[15] A. Sanyal, A. Gupta, H.H. Bayraktar, R.Y. Kwon, T.M. Keaveny. Shear strength behavior of human trabecular bone. Journal of Biomechanics, 45, 2513-2519, (2012). https://doi.org/10.1016/j.jbiomech.2012.07.023

[16] S.P. Väänänen, L. Grassid, G. Lorenzo, G. J.S. Flivike, J.S, Jurvelina., H. Isaksson, Generation of 3D shape, density, cortical thickness and finite element mesh of proximal femur froma DXA image, Medical Image Analysis,24, 125-134, (2015). https://doi.org/10.1016/j.media.2015.06.001